AD-A100 860 SRI INTERNATIONAL MENLO PARK CA F/G 17/1
STUDY OF REMOTE WIND MEASUREMENT USING ACOUSTIC ANGLE-OF-ARRIVA--ETC(U)
APR 81 P B RUSSELL, E M LISTON, S A DELATEUR DAAG29-78-C-0009
UNCLASSIFIED ARO-13850.1-GS NL

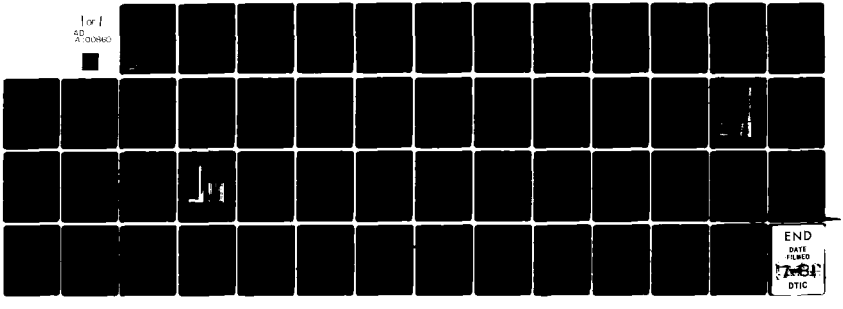

ARO 13850.1-GS

AD A100860

STUDY OF REMOTE WIND MEASUREMENT USING ACOUSTIC ANGLE-OF-ARRIVAL TECHNIQUES

(12) LEVEL II

Final Report

April 1981

By: Philip B. Russell, Senior Physicist
Edward M. Liston, Senior Chemical Engineer
Stephen A. DeLateur, Research Engineer
Atmospheric Science Center

Prepared for:

U.S. Army Research Office
Geosciences Division
Research Triangle Park, North Carolina 27709

Contract DAAG29-78-C-0009

DTIC
ELECTE
JUN 30 1981
S D
B

SRI Project 7245

DISTRIBUTION STATEMENT A
Approved for public release;
Distribution Unlimited

DTIC FILE COPY

SRI International
333 Ravenswood Avenue
Menlo Park, California 94025
(415) 326-6200
Cable: SRI INTL MPK
TWX: 910-373-1246

UNCLASSIFIED
SECURITY CLASSIFICATION OF THIS PAGE (When Data Entered)

REPORT DOCUMENTATION PAGE

READ INSTRUCTIONS BEFORE COMPLETING FORM

1. REPORT NUMBER

2. GOVT ACCESSION NO. AD-A100 866

3. RECIPIENT'S CATALOG NUMBER

4. TITLE (and Subtitle)

STUDY OF REMOTE WIND MEASUREMENT USING ANGLE-OF-ARRIVAL TECHNIQUES
ACOUSTIC

5. TYPE OF REPORT & PERIOD COVERED

Final Report
Mar 78 — Feb 81

6. PERFORMING ORG. REPORT NUMBER

Final Report, SRI Project 7245

7. AUTHOR(s)

Philip B. Russell, Edward M. Liston, and Stephen A. DeLateur

8. CONTRACT OR GRANT NUMBER(s)

Contract DAAG29-78-C-0009

9. PERFORMING ORGANIZATION NAME AND ADDRESS

SRI International
333 Ravenswood Avenue
Menlo Park, California 94025

10. PROGRAM ELEMENT, PROJECT, TASK AREA & WORK UNIT NUMBERS

11. CONTROLLING OFFICE NAME AND ADDRESS

U.S. Army Research Office
Post Office Box 12211
Research Triangle Park, North Carolina 27709

12. REPORT DATE
April 1981

13. NO. OF PAGES
45

14. MONITORING AGENCY NAME & ADDRESS (if diff. from Controlling Office)

15. SECURITY CLASS. (of this report)

Unclassified

15a. DECLASSIFICATION/DOWNGRADING SCHEDULE

16. DISTRIBUTION STATEMENT (of this report)

Approved for public release; distribution unlimited.

17. DISTRIBUTION STATEMENT (of the abstract entered in Block 20, if different from report)

NA

18. SUPPLEMENTARY NOTES

The view, opinions, and/or findings contained in this report are those of the author(s) and should not be construed as an official Department of the Army position, policy, or decision, unless so designated by other documentation.

19. KEY WORDS (Continue on reverse side if necessary and identify by block number)

20. ABSTRACT (Continue on reverse side if necessary and identify by block number)

An angle-of-arrival sodar system was designed, built, and tested with the goal of determining boundary-layer winds. The system measures the backscattered signal induced in two closely spaced microphones on a single parabolic receiver antenna; the angle of arrival is calculated from the relative signal amplitudes. This is the acoustic analog of the amplitude-monopulse radar technique. However, the acoustic system uses distributed (atmospheric) targets and a fixed (not steerable) antenna.

Tests demonstrated that the system can receive atmospheric echoes and process the analog signals to estimate angle-of-arrival (hence, layer-averaged wind) when signal-to-noise ratios are adequate. However, the validity of these wind estimates was not demonstrated with correlative wind data. Digital processing techniques were

DD FORM 1 JAN 73 1473
EDITION OF 1 NOV 65 IS OBSOLETE

UNCLASSIFIED
SECURITY CLASSIFICATION OF THIS PAGE (When Data Entered)

20. ABSTRACT (Continued)

implemented with the goals of automatic wind calculation, identification of adequate signal-to-noise ratios, and noise subtraction. Computer hardware limitations prevented achieving these goals. However, we believe that they could be achieved by using a computer with larger memory capacity.

CONTENTS

ILLUSTRATIONS

SUMMARY

An angle-of-arrival sodar system was designed, built, and tested with the goal of determining boundary-layer winds. The system measures the backscattered signal induced in two closely spaced microphones on a single parabolic receiver antenna; the angle of arrival is calculated from the relative signal amplitudes. This is the acoustic analog of the amplitude-monopulse radar technique. However, the acoustic system uses distributed (atmospheric) targets and a fixed (not steerable) antenna.

Tests demonstrated that the system can receive atmospheric echoes and process the analog signals to estimate angle-of-arrival (hence, layer-averaged wind) when signal-to-noise ratios are adequate. However, the validity of these wind estimates was not demonstrated with correlative wind data. Digital processing techniques were implemented with the goals of automatic wind calculation, identification of adequate signal-to-noise ratios, and noise subtraction. Computer hardware limitations prevented achieving these goals. However, we believe that they could be achieved by using a computer with larger memory capacity.

I INTRODUCTION

A. Boundary Layer Winds

A variety of Army activities require information on winds in the planetary boundary layer. For example, low-altitude paradrop and bombing missions can be critically affected by variable winds aloft. For these applications, knowledge of the vertically integrated boundary-layer wind (Air Weather Service 1971; Cormier 1975)* could greatly improve the effectiveness of operations. Ballistic and rocket launching operations also require information on the vertical wind structure. Ideally, data on the wind effect over the projectile's total trajectory should be available immediately before firing, so that appropriate corrections can be applied. For current practical purposes, it would be highly advantageous to provide wind data for the layers in the immediate vicinity of a weapon system, within one minute of firing, and to heights of about 500 ft (150 m). Such wind data could be in the form of a layer-mean wind vector. The ability to make such measurements with a simple field-transportable device could serve as a point of departure for further developments, such as extension of the technique to higher levels.

In addition to the operational needs just mentioned, the Army's Automatic Meteorological System (Swingle, 1969) will have a major need for small-scale atmospheric wind data. Such data are required as inputs to mesoscale and microscale predictions. Current operational, ground-based Army equipment cannot provide the required winds-aloft data. Significant improvements in prediction cannot be expected until improved techniques become available to measure the required atmospheric input parameters, including winds aloft.

---

*References are listed at the end of the report.

B. The Acoustic Angle-of-Arrival Technique

The acoustic angle-of-arrival technique works by transmitting a pulse of sound near-vertically into the atmosphere and measuring the way that winds transport the pulse in the horizontal. Figure 1 shows the basic geometry. For a pulse backscattered at height h, it can be shown (McAllister, 1971a,b; Georges and Clifford, 1972; Mahoney, 1974; Mahoney et al., 1973; Peters et al., 1978) that sound arriving back at the transmitting antenna has its wavefront normal tilted by a angle θ with respect to the vertical, with components given by

$$\{\theta_x(h),\ \theta_y(h)\} = \frac{2}{c}\{\bar{u}(h),\ \bar{v}(h)\} \tag{1}$$

where θ is in radians, c is the speed of sound ($c \gg u,v$),

$$\{\bar{u}(h),\ \bar{v}(h)\} = \frac{1}{h}\int_0^h \{u(z),\ v(z)\}\ dz\ , \tag{2}$$

and u(z), v(z) are the x and y components of the wind at height z. Hence, a measurement of the angle of arrival $\{\theta_x(h),\ \theta_y(h)\}$ provides a measure of the mean wind between the surface and height h. The wind in a lamina of thickness Δh can in principle be obtained by evaluating the difference in angle-of-arrival measurements; that is, if we define

$$\{\bar{u}(h,\Delta h),\ \bar{v}(h,\Delta h)\} \equiv \frac{1}{\Delta h}\int_h^{h+\Delta h} \{u(z),\ v(z)\}\ dz\ , \tag{3}$$

we have [by Eqs. (1) and (2)]

$$\{\bar{u}(h,\Delta h),\ \bar{v}(h,\Delta h)\} = \frac{c}{2\Delta h}\Big|h\{\theta_x(h),\theta_y(h)\} - (h+\Delta h)\{\theta_x(h+\Delta h),\ \theta_z(h+\Delta)\}\Big|\ . \tag{4}$$

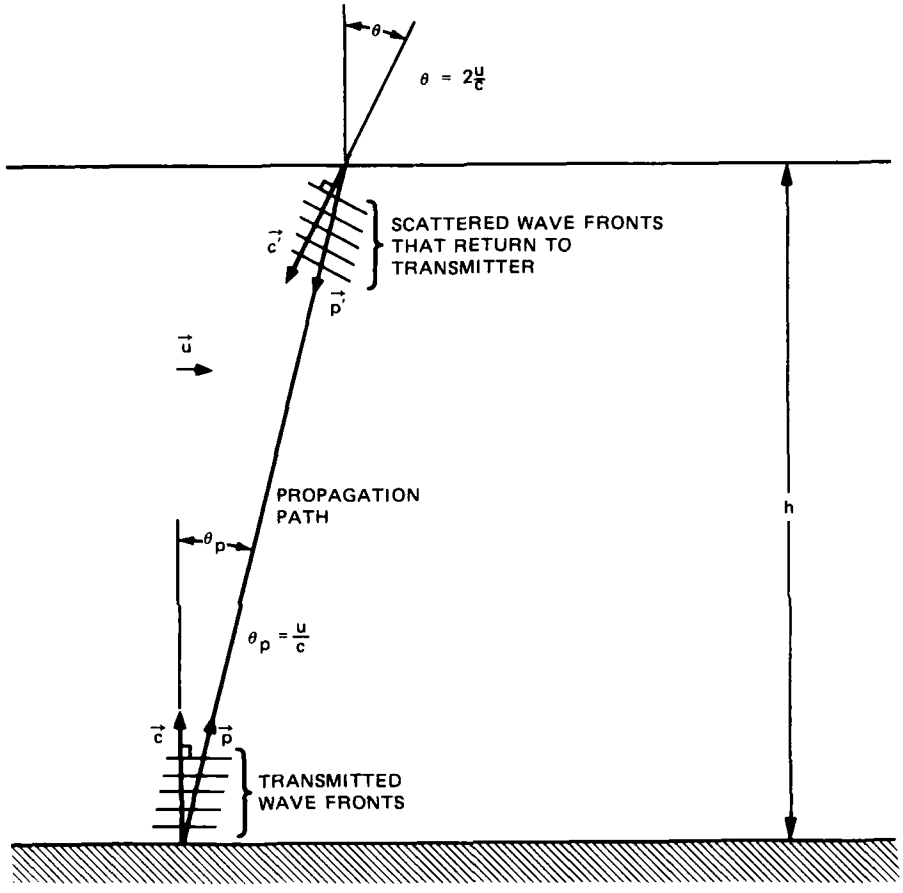

FIGURE 1 BASIC GEOMETRY OF THE ACOUSTIC ANGLE-OF-ARRIVAL WIND-SENSING TECHNIQUE

Propagation vector $\vec{p}$ (in the ground frame of reference) is the resultant of the wave front vector $\vec{c}$ (in the moving frame of reference) and the wind velocity vector $\vec{u}$ (in ground frame of reference). Propagation path shown assumes wind velocity $\vec{u}$ independent of height. Primed quantities refer to scattered waves.

The angle of arrival (θ_x, θ_y) can be determined by measuring either the phase difference or the amplitude difference between signals induced in closely spaced receiver channels. The phase difference results from the fact that the wave fronts are tilted at angle (θ_x, θ_y) with respect to the horizontal. Hence, for sound of wavelength λ and receiver channels spaced by distance (d_x, d_y), a phase lag of

$$(\phi_x, \phi_y) = \frac{2\pi}{\lambda} (d_x \sin\theta_x, d_y \sin\theta_y) \tag{5}$$

is induced between adjacent channels. The phase-based technique of measuring acoustic angle of arrival has been implemented by McAllister (1971a,b) and by Peters et al. (1978).

If two microphones are mounted in the focal plane of the same parabolic dish, with each microphone offset from the axis of the dish by a small distance, the receiver beam pattern shown in Figure 2 will result. The sensitivity functions $R_1(\theta)$ and $R_2(\theta)$ will each be tilted away from the axis by the "squint angle" q_x. Hence, signals arriving at angle (θ_x, θ_y) with respect to the vertical induce different amplitudes in the two receiver channels. The amplitude difference contains information on both the magnitude and the sign of the angle of arrival (θ_x, θ_y). This tilted-pattern/amplitude-difference method of measuring angle-of-arrival is the basis of the monopulse tracking technique, which has been implemented in many microwave radar systems (e.g., Rhodes, 1959; Skolnick, 1970). However, at the start of this project it had not, to our knowledge, been implemented in an acoustic radar system.

C. Relationship to the Acoustic Doppler Technique

Because the frequency of the received acoustic signal is Doppler-shifted by the wind in the scattering volume, acoustic radar wind measurements can also be made by Doppler analysis of the received signal frequency. Many papers have described the principles and practice of acoustic Doppler wind measurements (e.g., Beran et al., 1974; Hall et al., 1975; Peters et al., 1978), and several commercial systems are

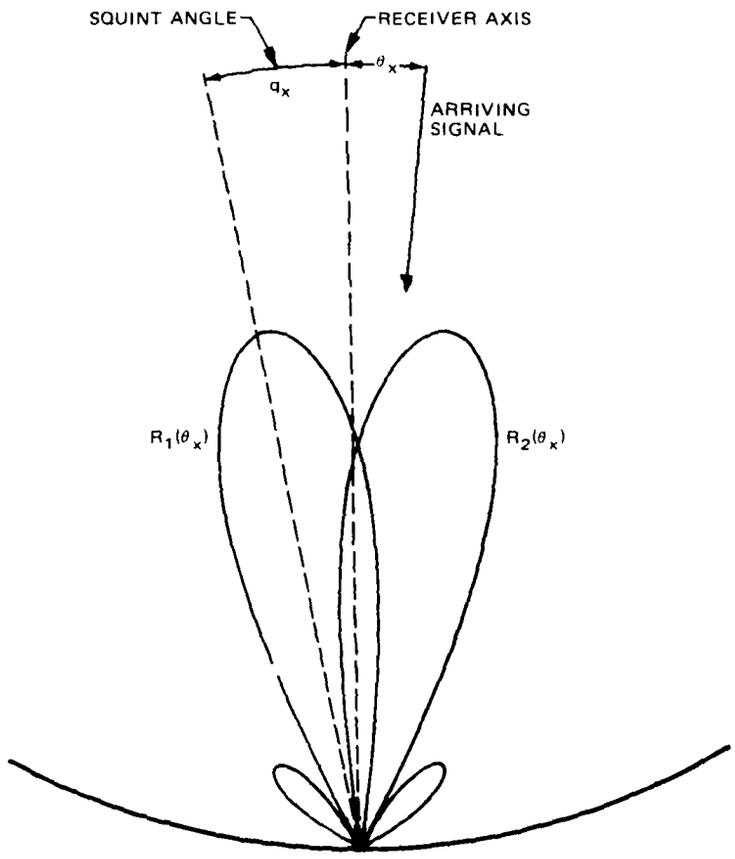

FIGURE 2 ANGLE-OF-ARRIVAL MEASUREMENT TERMINOLOGY USING AMPLITUDE COMPARISON AND TILTED RECEIVER CHANNEL BEAMS

available. At the start of this project, Doppler acoustic radar systems described in the literature used a transmit/receive configuration with three widely spaced antennas (100 m apart) to measure both horizontal wind components with good signal-to-noise ratio. An advantage of the tristatic Doppler system is the ability to measure directly {u(z), v(z)} profiles [rather than layer averages {$\bar{u}$(h), $\bar{v}$(h)}] and to obtain strong signals from unstable and neutral atmospheric regions by using scattered angles other than near 180°. (At scattering angles near 180°, as obtained in a monostatic configuration, the strongest signals are obtained only where the temperature profile is stable and in the lower parts of convective plumes--see e.g., Hall, 1972; Wycoff et al., 1973.) However, a major weakness of the tristatic Doppler system is the need for three widely spaced, mutually aligned antennas. This need severely limits the portability of such systems, requires long setup times, and restricts the number of suitable locations. In contrast, the acoustic angle-of-arrival technique can provide measurement of both horizontal wind components (albeit layer-averaged) from a single (multichannel) antenna. Thus, this angle-of-arrival project was undertaken with the goal of developing an acoustic wind sensor that would be more portable and convenient than the Doppler systems described in the literature up to about 1977.

During the course of this project, improvements (made elsewhere) in Doppler acoustic radar systems greatly increased portability and convenience. Therefore, a midproject review of the relative merits of existing Doppler and potential angle-of-arrival (AoA) systems was conducted in 1979. The results are summarized in Appendix A. The conclusion was that a system with a single vertical AoA antenna measuring profiles of the two horizontal wind components, or a single hybrid AoA-Doppler antenna measuring all three components, would have worthwhile advantages over the two- or three-antenna monostatic Doppler system required to make the same measurements. The primary advantage of the AoA or hybrid system would be operational (smaller bulk, better portability, less expensive construction and maintenance), although some advantages in information might also be available. However, it was

recognized that full achievement of this would entail solving several major problems associated with the AoA technique. The remainder of this report describes the SRI efforts implement and test the AoA technique.

II PROCEDURES AND RESULTS

A. First Year (March 1978-February 1979)

At the start of this project, we had planned to construct a planar-array antenna system to make phase-shift angle-of-arrival measurements. [see Eq. (3)]. Such a system would have been similar to those previously implemented by McAllister (1971a,b) in Australia and Peters et al. (1978) in Germany.

However, before construction, we reviewed the amplitude monopulse technique, its previous application in microwave radar systems, and its potential for use in acoustic wind sensing. On the basis of that review, we decided to implement the amplitude monopulse technique using a single parabolic dish antenna with the transmitter horn on axis and receiver microphones off axis. This design contrasts with the speaker-array type of antenna used by previous investigators. Our reasons for adopting the dish approach were:

- It made maximum use of the limited antenna space in the trailer-mounted acoustic enclosure used in this project.
- Construction was simplified through the use of fewer acoustic transducers.
- Larger antennas could be assembled using no more transducers--only a larger dish.
- Many microwave tracking radars use this design for angle-of-arrival measurements with good success.

Although the new acoustic design entailed some risk, we felt the risk was warranted for the reasons listed. In addition, we later realized that the amplitude-sensing technique has potential advantages over the phase-sensing technique in terms of noise subtraction (see Appendix A and the end of this section).

A dish antenna with two receiver channels (as shown in Figure 3) was constructed, along with transmitter electronics, two-channel receiver electronics, and a digital data system. An outdoor test facility was also constructed; this facility included a tower-mounted movable acoustic source, a tower-mounted u-v-w anemometer, and an acoustic enclosure for the antenna dish (on the ground). The source, mounted above the antenna, could be moved to $\pm 10^{o}$ off axis, using a pulley controlled from the ground, to calibrate the system's response to different acoustic angles of arrival.

After initial tests, microphone preamplifiers were added at the antenna to increase signal-to-noise ratios. Although analog circuits were assembled to measure the sum and difference of signal amplitudes in the two receiver channels, these preliminary circuits did not perform properly, and this approach was temporarily abandoned in favor of digital processing.

Most of the testing during the first year was accomplished in January and February 1979 during a visit by Dr. Gerhard Peters of the Max Planck Institute in Hamburg. Dr. Peters, who has developed and tested both Doppler and AoA systems in Hamburg (Peters et al., 1978), was a paid consultant to this project.

The sensitivity of each receiver channel was increased by about 10 dB by modifying the microphones and placing them in $\lambda/4$ resonant tubes. Because the resulting system was background-limited by noise in the SRI testing yard, no further sensitivity improvements were sought during the test period.

The relative gain of the two receiver channels was found to be unstable within about 3 dB. Although this instability is unacceptable for long-term AoA measurements using the amplitude-comparison technique, it was tolerated for the remainder of the first-year test period. Some shortcomings were found in the narrowband (commutating) filter and the electronic circuits for AoA detection. However, as both of these functions were also performed by software in the data-system computer,

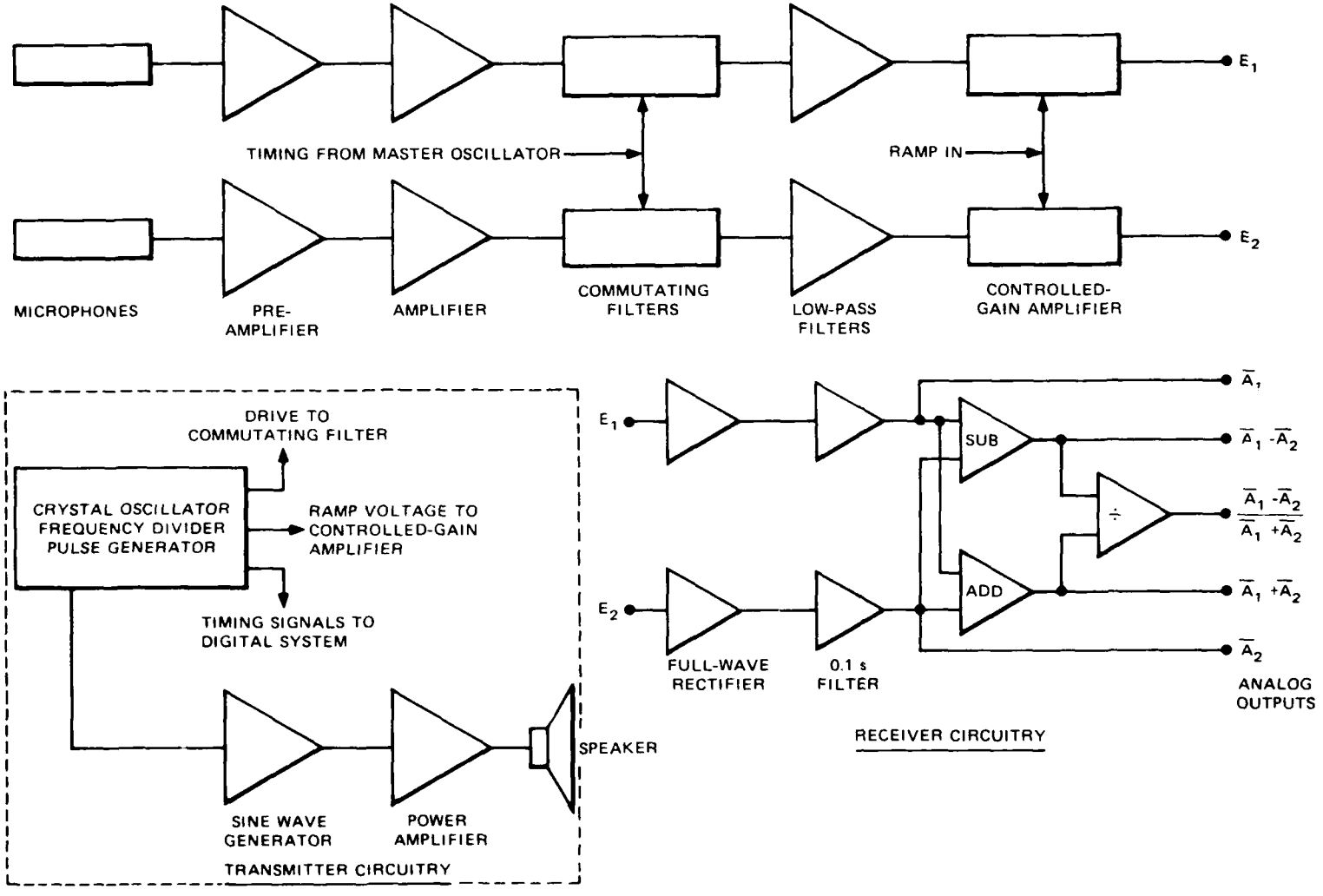

FIGURE 3 BLOCK DIAGRAM OF ANALOG CIRCUITRY

immediate circuit improvements were not sought. Real-time digital methods for filtering and AoA measurement gave tolerable results throughout this test period; however, a need for faster and more effective methods in the future was recognized.

The movable source above the antenna was used to measure the receiver beam pattern, $R_i(\theta)$, for each channel i (see Figure 2). In these first-year tests, the calculated squint angles were

$$q_1 = -q_2 = 6.7^\circ \tag{6}$$

resulting from a microphone separation of 6.7 inches (17 cm) and a dish focal length of 29 inches (74 cm). However, the measured patterns were not symmetric about the antenna axis ($\theta = 0$), and neither pattern peaked at the calculated squint angle, $\pm 6.7^\circ$. Instead, the measured squint angle was about $\pm 4^\circ$. The nonideal beam patterns were caused by reflections from the test-source tower as well as the transmitter horn. Despite the nonideal beam patterns, we were able to perform several useful tests with the first-year setup and deduce some fundamental difficulties and advantages of the acoustic amplitude monopulse technique.

An important difference between the acoustic monopulse technique for wind sensing and previous microwave radar monopulse tracking of point targets is the distributed nature of the target in the acoustic wind-sensing case. For the 6-ft (1.8-m) diameter dish and 1.0 to 1.6 kHz frequency used in our tests, the transmitted beamwidth is initially about 13° (FWHM); this width can increase through turbulent spreading as the pulse propagates through the atmosphere. Because of the inhomogeneous nature of thermal turbulence (the scattering "target" in the acoustic backscattering case), the source of backscattered sound is not uniformly distributed across the transmit beamwidth, but may consist of one or more "bright spots" located anywhere within the beamwidth. Thus, the acoustic target, instead of being located at a unique angle θ, is characterized by a "brightness distribution," $B(\theta)$. The amplitude A_i of

the signal-induced receiver channel i is the convolution of this brightness distribution with the channel beam pattern; hence,

$$A_i = \int B(\theta)\ R(\theta - q_i)\ d\theta \ , \tag{7}$$

where q_i is the squint angle on which the channel i beam pattern is centered. Note that in the case of a point target (or source) at θ_t, $B(\theta)$ reduces to the Dirac delta function $\delta(\theta_t)$, and Eq. (7) reduces to

$$A_i = \int \delta(\theta_t)\ R(\theta - q_i)\delta\theta = R(\theta_t - q_i) \ , \tag{8}$$

as expected. This is in fact how functions $R(\theta - q_i)$ were measured, using the movable point source (delta function) above the antenna.

The task of an amplitude-based angle-of-arrival wind sensor is to use the measured signal amplitudes, A_i, to infer something about the target brightness distribution, $B(\theta)$. Fortunately, it is not necessary to infer the complete function $B(\theta)$; instead we try to infer its centroid,

$$\theta_c = \int B(\theta)\ \theta\ d\theta \ / \int B(\theta)\ d\theta \ , \tag{9}$$

as being a good measure of the "true" angle of arrival. Our task is thus to construct some function of the A_i that is uniquely related to θ_c.

During the January-February 1979 tests two such functions were tried. The first,

$$f_1 = \frac{A_1 - A_2}{A_1 + A_2} \ , \tag{10}$$

is the usual difference-over-sum function used in microwave monopulse tracking radar (Rhodes, 1959; Skolnick, 1970). In tracking radar, where the antenna is steered using f_1 as a feedback signal, it is necessary only that $f_1 \rightarrow 0$ as $\theta_c \rightarrow 0$, and that f_1 change sign when θ_c does. However, in our application the antenna is fixed; hence, the exact shape of $f_1(\theta_c)$ must be known, so that f_1 can be inverted to obtain θ_c. We therefore measured f_1 as a function of θ_c, the position of the movable acoustic source.

The results of these preliminary measurements were fairly encouraging, indicating that f_1 could be inverted to yield θ_c over a range of roughly $\pm 4^{\circ}$. Using Eq. (1), this corresponds to a wind speed range of ± 11 m/s or ± 25 mi/h. Unfortunately, it was found that f_1 is sensitive to the background noise often present during field operations. To see this, note that, for nonnegligible noise, Eq. (7) must be modified to yield

$$A_i = S_i + N_i \ , \tag{11}$$

where N_i is the background noise in channel i and S_i is the backscattered signal,

$$S_i \equiv \int B(\theta)\ R(\theta - q_i)\ d\theta \ . \tag{12}$$

Hence, with noise inputs present in each receiver channel,

$$F_1 = \frac{S_1 - S_2 + N_1 - N_2}{S_1 + S_2 + N_1 + N_2} \tag{13}$$

When the tests at the SRI test site were repeated for low signal-to-noise ratios, the effects of noise in Eq. (13) were evident, noticeably distorting the f_1 vs θ_c relationship that had been obtained at high

signal-to-noise ratio. Thus, for nonnegligible background noise, f_1 is not a unique function of θ_c.

The background-noise problem with f_1 could potentially be solved by measuring N_i in each channel (just before pulse transmission) and subtracting it from A_i to obtain S_i. However, f_1 has an additional problem. Recall that, because of the 13^o transmit beamwidth (FWHM) and the possible occurrence of "bright spots" anywhere within the beam, θ_c can range from about $+6^o$ to -6^o on any given shot, even when no wind is blowing. Because the probability distribution of bright spots within the beam should be random, averaging θ_c over many shots should yield the mean wind-induced θ_c. However, determination of θ_c on a shot-by-shot basis is not possible using f_1 unless the range of θ_c over which f_1 is monotonic exceeds the transmit beamwidth plus the maximum wind-induced angle-of-arrival. If this is not the case, the inverse function $\theta_c(f_1)$ is not defined over the possible range of θ_c, and the many-shot average θ_c is not equal to $\theta_c(f_1)$.

Because of these problems with f_1, another function, f_2, was tested. f_2 is defined as

$$f_2 \equiv \frac{A_1^2 A_2^2}{E_1 \cdot E_2} \tag{14}$$

where E_i is the received vector signal in channel i, i.e.,

$$E_i = A_i \cos(\omega t - \phi_i) ,$$

where ω is the carrier frequency and ϕ_i is a phase angle. However, this function was abandoned because tests showed that

- Like f_1, $f_2(\theta_c)$ was also nonmonotonic over the range $\pm 6^o$ (with the 6.7 inches microphone spacing that was used in their early tests), so that the inverse, $\theta_c(f_2)$, was undefined.
- Noise can make the instantaneous denominator of f_2 zero or negative, making f_2 very unstable at low signal-to-noise ratios.

A third function,

$$f_3 \equiv \frac{q}{2} \frac{A_2 - A_1}{2A_3 - A_2 - A_1} \tag{15}$$

was also defined during the January-February 1979 test period. It was not tested then because f_3 requires a third receiving channel on the antenna axis. f_3 is promising because, if each channel beam pattern can be approximated by a parabola centered on its squint angle q_i, f_3 is equal to the centroid θ_c of the brightness distribution $B(\theta)$, for all angles over which the parabolic approximation is valid. To show this, we define the parabolic beam patterns as

$$R_1 = C - D(\theta + q)^2 \tag{16}$$

$$R_2 = C - D(\theta - q)^2 \tag{17}$$

$$R_3 = C - D\theta^2 \ . \tag{18}$$

Substituting these into Eq. (7) yields

$$A_2 - A_1 = 4Dq\theta_c B \tag{19}$$

$$2A_3 - A_2 - A_1 = 2Dq^2 B \ , \tag{20}$$

where we have used the definition Eq. (9) and

$$B \equiv \int B(\theta) d\theta \ . \tag{21}$$

Substituting Eqs. (19) and (20) into Eq. (15) yields

$$f_3 = \theta_c \ , \tag{22}$$

as desired. Hence, f_3 is a monotonic (thus invertible) function of θ_c for all angles that (approximately) satisfy Eqs. (16) through (18). Although Eqs. (16) through (18) will not be exact over all angles, they should be approximately correct over the range where each $R_1(\theta)$ is strong (i.e., the $\pm 6^o$ beam width). Thus, f_3 should at least be monotonic over a wider range of angles than f_1 or f_2, and, after empirical determination, invertible for θ_c.

All of the January-February 1979 tests described so far used the movable elevated acoustic source to characterize receiver response. Toward the end of the tests, the AoA sodar's response to atmospheric echoes was tested and found to be very poor. Thus, at the end of the first year, five tasks were defined for the second year. These were:

(1) Improve performance on atmospheric echoes.

(2) Correct gain drifts in receiver channels.

(3) Improve digital filtering and amplitude measurements.

(4) Improve acoustic enclosure and test-source mounting setup to eliminate echoes; locate at quieter site.

(5) Implement third receiver channel and test function f_3.

B. Second Year (March 1979-February 1980)

Very little technical effort was expended during the first nine months of the second year because funds were being conserved for a major effort that began near the end of the year and continued into the third year. For purposes of continuity, that effort is described Section II-C.

Several planning meetings were held during the second year to determine the future direction of the project. One of these meetings was held at the University of Hamburg while Dr. Russell, the Principal Investigator on this project, was visiting Germany on another project. The results of that meeting are described in Appendix A. As noted there, it was decided that the amplitude-sensing AoA technique had enough potential advantages over acoustic Doppler and phase-sensing AoA

techniques to warrant continuing the research, in particular by attacking the five tasks listed at the end of the previous section.

C. Third Year (March 1980-February 1981)

Both electronic and acoustic improvements were made to optimize performance on atmospheric echoes and to correct the gain drift in the receiver channels [Tasks (1) and (2) of the list in Section II-A]. The electronic improvements were made in the preamplifiers, the commutating filter, and the output (analog) channels. The preamplifiers were completely rebuilt to reduce noise, eliminate the signal gain drift, incorporate low-noise power supplies, incorporate passive narrowband filters, and improve the input impedance matching. These improvements, along with improvements in the microphone housing, reduced the electronic noise to well below the background acoustic noise, even in quiet locations.

The commutating filter (an active narrow-band filter) was rebuilt as a 16-pole filter. The advantages over the previous four-pole filter are reduced sensitivity to incoming signal phase shifts and simplified filtering of switching harmonics (now at 16 kHz for a 1 kHz signal). The FWHM bandwidth is 30 Hz at the 1600 Hz center frequency.

Provisions were made to record the following output analog signals:

- Ramp-gain amplified amplitudes, E_1 and E_2
- A_1 and A_2 with 0.1-s smoothing
- $\bar{A}_1 - \bar{A}_2$
- $\bar{A}_1 + \bar{A}_2$
- $(\bar{A}_1 - \bar{A}_2)/(\bar{A}_1 + \bar{A}_2)$
- Trigger and timing data for the digital system.

The block diagram for the resulting system is shown in Figure 3. See Appendix B for a further discussion of the analog and digital circuitry.

The ability of this system to detect atmospheric echoes was demonstrated by comparing the output of the SRI system with that of a commercially available unit (AeroVironment). These data are shown in Figure 4. The first, third, and fourth blocks of data are from the SRI unit. The second block of data is from the commercial unit. Note that the SRI system readily detects echoes from both inversions and convective plumes. Although the SRI system appears to show more noise than the AeroVironment at high altitudes, tests revealed that the difference was caused by an AeroVironment ramp gain that increased less rapidly than the desired linear function.

Because the SRI site used for these tests was quite noisy, the system was moved to a quieter location at Stanford University. All of the following data were taken at that site.

The receiver beam patterns were measured by suspending a small sound source 21 ft (6.4 m) over the receiver dish and moving the sound source across the axis of the receiver when no wind was blowing. This sound source was driven by the commutating-filter oscillator to ensure that the received signal was at the peak of the filter response.

The first measurement made with the new system used a single transmit/receive antenna dish, with the transmitter horn mounted on axis and the receiver microphones mounted off axis on either side of the horn. Tests showed that there were large sidelobes in the receiver patterns, caused by reflections from the walls of the transmitting horn. To eliminate these sidelobes and the associated distortion of f_1, it was necessary to separate the transmitter and receiver. The transmitter horn was mounted over a 6-ft (1.8-m) dish and placed inside an acoustic enclosure beside the trailer containing the receiver dish and microphone.

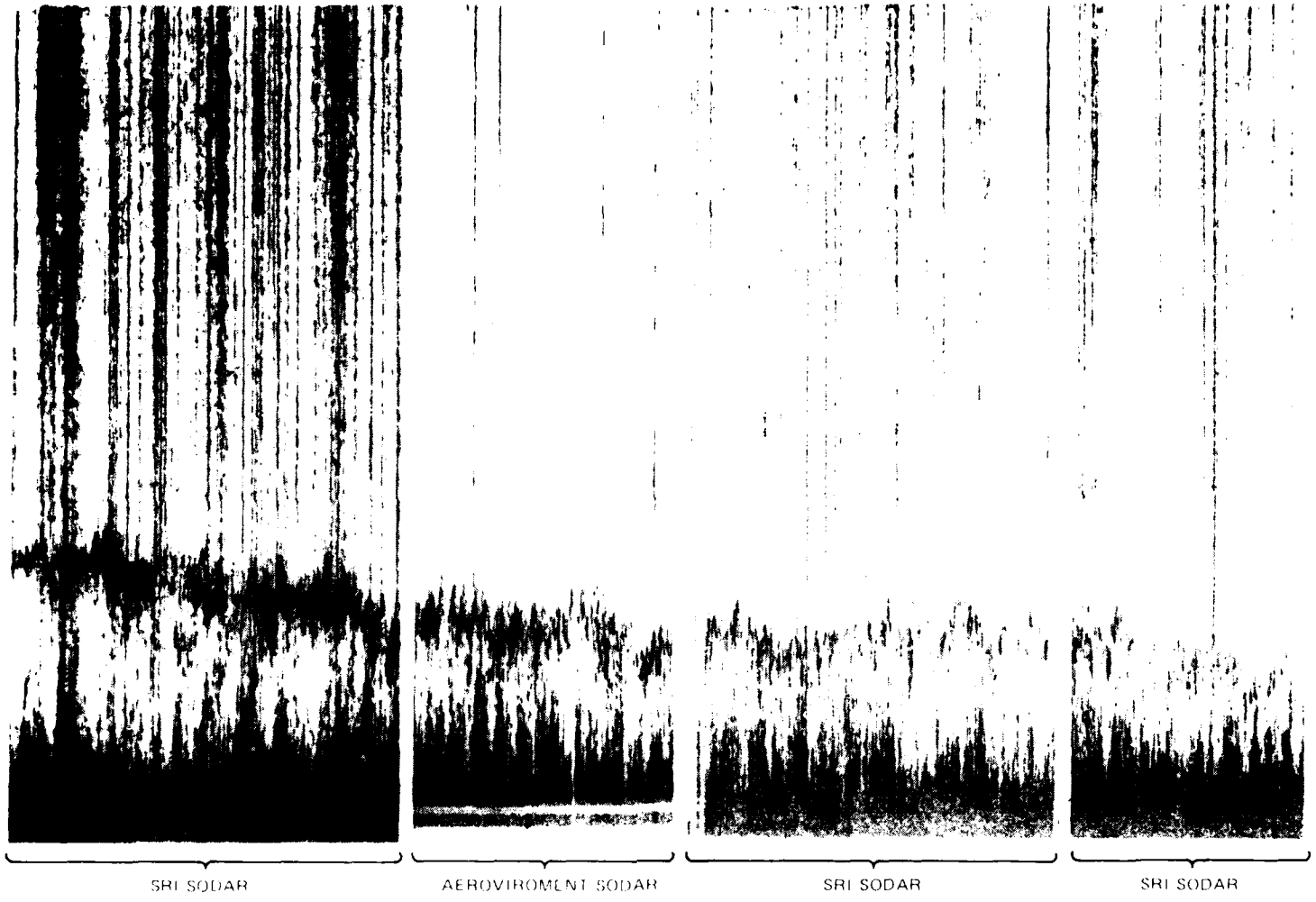

FIGURE 4 COMPARATIVE SODAR DATA

The two microphones were initially placed 6 inches (15 cm) apart at the correct focal distance from the dish. The measured response pattern for this configuration is shown in Figure 5. Figure 6 is the function

$$f_1 = \frac{A_1 - A_2}{A_1 + A_2}$$

calculated from the data in Figure 5. Note that f_1 is nearly linear for $|\theta_t| \leq 4^o$, with the inverse function given by $\theta_t(\text{deg}) = 4.14 f_1$.

Inspection of these data indicates that the limits of the linear relationship are set by the amount of overlap of the two patterns $R_1(\theta)$ and $R_2(\theta)$ and the separation of the minima between the major lobe and the first sidelobe (see Figure 5).

To test this observation, the microphone spacing was successively set at 4, 3, and 2 inches (10.1, 7.6, and 5.1 cm) during a calm period. At each spacing, the sound source was moved across the receiver beam, and the function f_1 from the analog output was recorded. The response pattern for the 2 inch (5.1 cm) spacing is shown in Figure 7. Note that the near-linear, monotonic portion of f_1 is approximately 14^o wide. Thus, even if "bright spots" are present within the $\pm 6^o$ transmit beamwidth, these bright spots should still be within the monotonic (invertible) range of f_1 [cf. the discussion near Eq. (6)], provided a 2-inch (5.1-cm) spacing is used and the wind-induced angle of arrival does not exceed about 7^o (i.e., wind speeds do not exceed 21 m/s).

During this phase of the testing, an aircraft flew over the test site and the analog output of f_1 was recorded. Although the aircraft's position was not measured independently, the response of the system appeare to be almost identical to that found when the sound source was used. This showed that the response was not an artifact of the sound source.

Figure 8 shows the analog output data from atmospheric echoes using the SRI sodar. Figure 8(a) is the usual facsimile recording in which

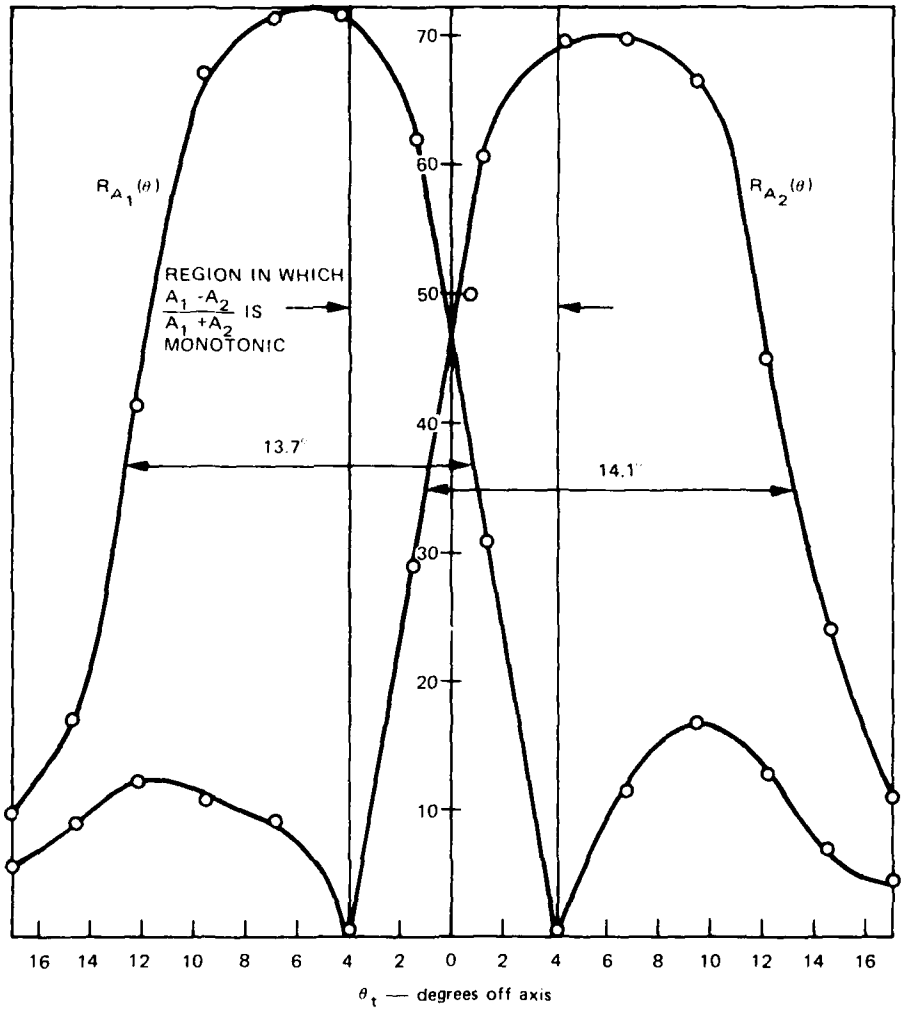

FIGURE 5 RESPONSE PATTERN FOR MICROPHONES WITH 6-INCH SPACING

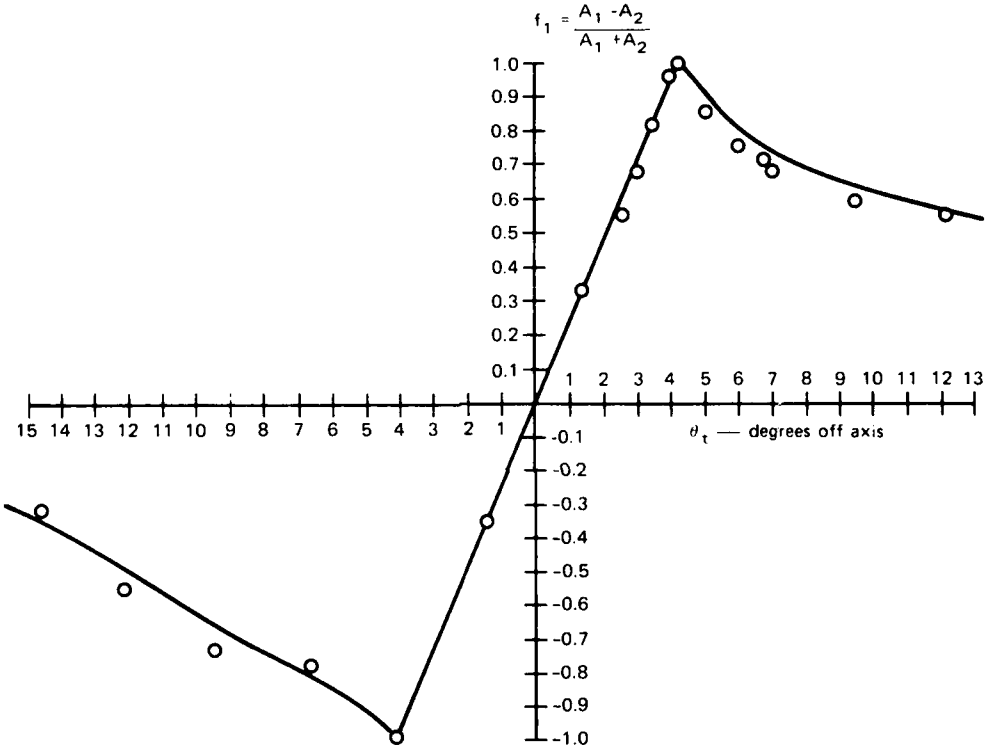

FIGURE 6 CALCULATED f_1 FROM DATA IN FIGURE 5

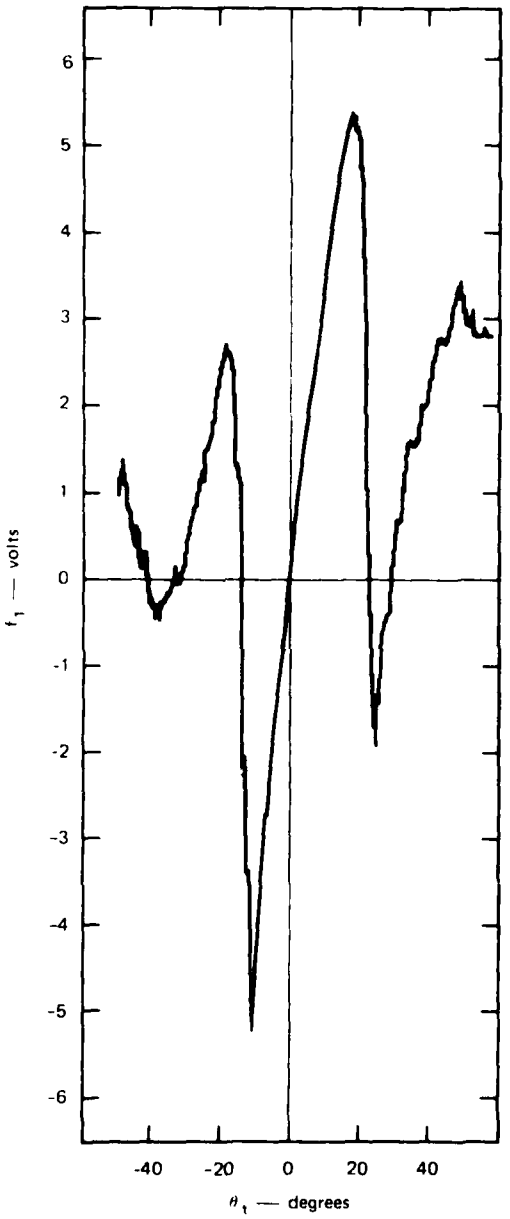

FIGURE 7 ANALOG f_1 RESPONSE PATTERN · · 2-INCH MICROPHONE SPACING

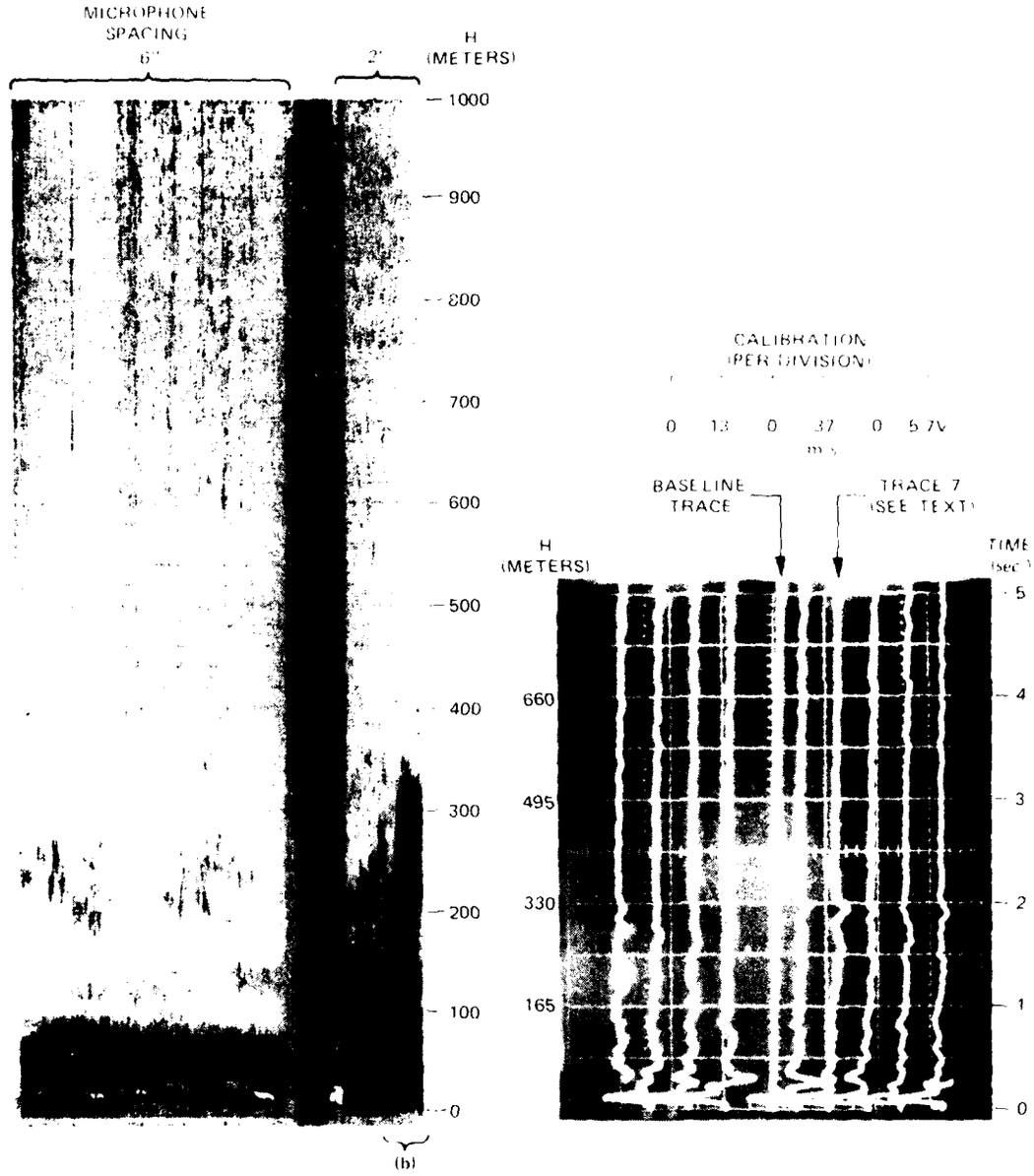

(a) FACIMILE RECORD OF SUM SIGNAL

(b) OSCILLOSCOPE RECORD OF ANALOG f_1 OUTPUT

FIGURE 4 OUTPUT DATA FROM SRI ANGLE-OF-ARRIVAL SODAR

the magnitude of the return signal is displayed as a function of height. Note that the data on the left side of this record were taken with the microphone spacing at 6 inches. The data on the right side were for a spacing of 2 inches. The intensity of the return signal increased because the microphones were closer to the focal point and the dish is more efficient at that point.

Figure 8(b) shows the oscilloscope record of f_1 for nine successive sodar soundings. [This record was made by putting a slowly increasing voltage on the horizontal axis so each trace is displaced to the right of the previous one.] The fifth trace is a baseline trace; note that it slopes to the right. The soundings were made 20 s apart. The calibration is 13^{o}/div or 37 m/s per division.

The data in Figure 8(b) correspond to the data at the right edge of Figure 8(a). Note that in Figure 8(b) there is a fairly consistent peak in f_1 at about 1.9 s, or a height of 315 m. Figure 8(a) also shows a strong return signal with a top at 315 m. Hence, the peak in f_1 occurs at a height where signal-to-noise ratio is large [cf. the discussion near Eq. (10)].

The average windspeed parallel to the microphone (x) axis was calculated from trace 7 in Figure 8(b) as follows:

- $f_1 = 1.8$ V (at 1.9 s)
- $\theta_x = 2.3^{o} \times f_1$ (V)
- $\bar{u} = 1/2\ \theta_x$ (rad) c
- c = 328 m/s;

thus,

$$\theta_x = 4.1^{o}$$

and

$$\bar{u} = 11.9 \text{ m/s}.$$

Whereas this is a reasonable value for the mean wind x component between the ground and 315 m, we were unable to confirm its validity, because simultaneous pilot-balloon wind measurements were not made, and no tower-mounted anemometers were available at the site. Also, no ground-based anemometer measurements were made, because the test site was in hilly terrain and it was felt that ground-level winds would be poorly correlated with vertically averaged winds.

Figure 8(b) also demonstrates some other difficulties that remain to be overcome with this AoA sodar. Note first that f_1(315 m) varies considerably from shot to shot, ranging from about 0 in Trace 8 to the maximum 1.8 V in Trace 7. It is doubtful that the vertically averaged wind (x-component) between the ground and 315 m is changing from 0 to 12 m/s over the 20-s shot-to-shot time difference. There are two probable reasons for the fluctuations in f_1(315 m):

- Shot-to-shot changes in the backscatter distributions, $B(\theta)$, within the 13° FWHM transmit beam.
- Large shot-to-shot variations in signal-to-noise ratio at 315 m. Both these effects are discussed at greater length in Section II-A.

The first effect could evidently be countered by averaging, for a series of shots, the θ_x value inferred from f_1(315 m) on each shot. The resulting average can be expected to have greatly reduced effects of the varying brightness distribution, because all measured f_1(315 m) values are within the monotonic f_1 vs θ_x range, and the brightness distribution, $B(\theta)$, should vary randomly within the beamwidth from shot to shot. However, shot-to-shot averaging will not counter the second effect because:

- Background noise itself can be anisotropic and correlated from shot to shot.
- The f_1 vs θ_x relationship is a function of noise whenever noise is nonnegligible compared to the backscattered signal [see Eq. (12) and discussion].

Thus, satisfactory processing requires a means of measuring background noise in each channel (just before pulse transmission) and either

subtracting this noise or excluding from angle-of-arrival calculations any parts of the signal that have poor signal-to-noise ratio.

Small signal-to-noise ratios might also explain some features in the vertical dependence of $f_1(z)$ shown in Figure 8(b). Note the consistently small values of f_1(295 m) just below the 315 m peak. If these values had been obtained at large signal-to-noise ratio [as most of the f_1(315m) values were], they would imply very small average wind between the surface and 295 m, and hence very strong wind shear between 295 and 315 m--i.e., a jet at 315 m. However, inspection of the sum output, $A_1 + A_2$, on the facsimile record [Figure 8(a)] reveals that the sum had very small signal-to-noise ratio at 295 m, thus, invalidating any inference of θ_x from f_1 at that height.

It is evident that obtaining useful wind estimates from this sodar system requires

- Shot-by-shot noise identification (or subtraction)
- Definition of signal-to-noise ratio as a function of range
- Multi-shot averaging of the high-signal inferred angles-of-arrival.

It was for these purposes (plus digital calculations of A_1, A_2, f_1, and θ_x) that we included a microcomputer-based digital data system as part of the sodar. However, it turned out that computer memory limitations prevented implementation of the second process listed above, and even prevented satisfactory determination of the range at which maximum signal occurred on each shot. Appendix B discusses the digital processing that was implemented and the difficulties that were encountered.

III DISCUSSION

The goal of this project has been to produce and validate a highly portable remote sensor of winds aloft using a technique (phase-sensing of acoustic angle of arrival) that had previously been described in the literature but not validated in the practical sense. Early in the project, we modified the method of approach to use amplitude-sensing of angles because of several anticipated advantages having mostly to do with hardware (see Section II-A).

Although the project did not produce a validated, highly portable sensor, some valuable information was gained. In particular, the results show promise for the amplitude-based acoustic angle-of-arrival technique, even using the relatively simple difference-over-sum function.

$$f_1 = \frac{A_1 - A_2}{A_1 + A_2} .$$

The monotonic range of this function can be made large enough (while still retaining sufficient sensitivity to angle) to span the fluctuations in angle of arrival that result from the distributed and inhomogeneous nature of the atmospheric acoustic target (i.e., the brightness distribution discussed in Sections II-A and II-C). Thus, the three-channel function f_3 described in Section II-A may not be necessary.

Moreover, the amplitude AoA technique has an inherent advantage over the phase AoA technique in terms of noise subtraction. That is, both amplitude AoA and phase AoA measurements fail when background noise becomes comparable to the backscattered signal. However, in the amplitude AoA technique, noise effects can potentially be reduced by

subtracting the noise amplitude in each receiver channel. There is no analogous phase-noise subtraction procedure.

Demonstrating the validity of the amplitude AoA technique requires two advances:

- Implementation of digital noise-subtraction, data-selection, and data-averaging techniques.
- Successful comparisons with direct wind measurements under a variety of conditions.

Appendix A

COMPARATIVE EVALUATION OF DOPPLER AND ANGLE-OF-ARRIVAL SODAR WING-SENSING TECHNIQUES

Appendix A

COMPARATIVE EVALUATION OF DOPPLER AND ANGLE-OF-ARRIVAL SODAR WIND-SENSING TECHNIQUES

In July 1979, at approximately the midpoint of this project, Dr. Russell (Principal Investigator for this project) and Dr. Gerhard Peters (Principal Investigator for the University of Hamburg's Doppler and angle-of-arrival sodar projects, and a consultant to this project) compared the perceived future for angle-of-arrival (AoA) measurements and the future for Doppler measurements. To initiate the discussion, they prepared lists of AoA advantages and disadvantages--both as perceived in 1975 when SRI's proposal to ARO was written) and as perceived in 1979. Tables A-1 and A-2 show the lists. In sum, although substantial progress with AoA measurements was made in 1975-79 (largely by Dr. Peters' group), much more progress was made with Doppler. Hence, the 1975 gap between Doppler and AoA had widened, rather than narrowed.

The review concluded by trying to answer the following question: "Can one expect to gain from AoA any operational advantage or valuable information (on wind, turbulence, or sodar technique) that cannot be achieved with Doppler?" The conclusion was that a system with a single vertical AoA antenna, measuring profiles of the two horizontal wind components, would have worthwhile advantages over the two- or three-antenna monostatic Doppler system required to make the same measurements. The primary advantage of the AoA or hybrid system would be operational (smaller bulk, better portability, less expensive construction and maintenance), although some advantages in information might also be available (see Advantages 3-5 of Table A-1). However, full achievement of this entails removing disadvantage 1a of Table A-2--that is, achieving good AoA results in the convective region below an elevated inversion. (See also advantage 6 of Exhibit 1 and disadvantage 1 of Table

Table A-1

ADVANTAGES OF AoA SODAR (RELATIVE TO DOPPLER), AS PERCEIVED IN 1975 AND 1979

1975 Perception	1979 Perception	Net Change
1. AoA potentially much more compact and portable than existing tristatic or bistatic Doppler systems.	AoA still more portable than tristatic or bistatic Doppler. But dual and trimonostatic Doppler systems are now proven and nearly as portable as AoA.	AoA advantage greatly reduced.
2. AoA able to get boundary-layer-average wind below inversion, whereas monostatic Doppler might not because of weak backscatter.	Measurements show ample backscattering in convective region below elevated inversions. Hence monstatic Doppler can also get averaged wind through boundary layer.	AoA advantage lost.
3. AoA measures the two horizontal components in the same value, whereas collocated dual monostatic Doppler antennas cannot.	True, but of practical advantage only in complex terrain, where spatial differences persist in time averages. Not superior for short time-scale studies, because AoA does not have required spatial resolution.	AoA advantage limited.
4. For AoA, vertical component information is not necessary to separate out horizontal components.	Still true.	AoA advantage holds.
5. AoA receiver bandwidth can be narrower, and antenna is vertical; hence AoA is potentially less sensitive to noise than Doppler (other factors being equal).	Still true. But this is only one aspect of overall sensitivity and operational effectiveness. Doppler successful in many situations. No direct comparisons available.	AoA advantage not demonstrated.
6. Single antenna could give boundary-layer-averaged horizontal wind (AoA) and vertical fluctuations (Doppler) as required for dispersion studies.	Collocated three-antenna monostatic Doppler could do same thing and be fairly portable and compact.	AoA advantage reduced.

Table A-2

DISADVANTAGES OF AoA SODAR (RELATIVE TO DOPPLER), AS PERCEIVED IN 1975 AND 1979

1975 Perception	1979 Perception	Net Change
1. AoA measures vertically-averaged wind, rather than vertically resolved.	Still holds, but inverting average profile to get vertically resolved profile is not necessarily subject to large errors.	AoA disadvantage holds.
1a. Since strength of backscatter signals below inversions questionable in 1975, not clear that AoA measurements could be obtained below inversion for differentiation to get vertical wind profile.	Peters has shown ample signal below elevated inversion; Doppler processing of these signals is successful, but AoA processing is not yet.	AoA disadvantage potentially beatable, but not yet beaten.
2. No demonstrated proof or comparisons with in-situ measurements of vertically averaged winds.	Peters comparisons successful within ground-based and elevated inversions. However, no satisfactory results outside of inversions. Also, results in inversions bot as satisfactory as Doppler.	AoA disadvantage reduced, but Doppler progress equal or better.
3. Potentially more susceptible to phase distortion than Doppler. (However, results of Brown and Keeler looked favorable.)	Still holds.	AoA disadvantage still a potential problem.

A-2.) In this connection, Dr. Peters felt that the amplitude AoA technique pursued at SRI may have substantial advantages over the phase AoA technique used up to 1979 by the University of Hamburg. This is because ambient acoustic noise measured in the various receiver channels is always correlated to some extent, and this produces some significant, though spurious, angle of arrival, especially when signal-to-noise ratio is in the neighborhood of 1. The amplitude AoA technique can remove correlated noise by subtraction in each channel, because the amplitude measured by each channel is a linear combination of signal and noise. There is no analogous "phase subtraction" procedure, because the phase in each channel is not such a linear combination.

Because of these potential advantages of the amplitude AoA technique, the SRI research was continued along the lines described in Section II-C of the text.

Appendix B

DIGITAL SIGNAL PROCESSING

Appendix B

DIGITAL SIGNAL PROCESSING

1. Equipment

The digital signal processing equipment is shown in Figure B-1. The system is built around a Digital Equipment Corp. PDP-11/03 computer, which contains an LSI-11 microcomputer, 32K bytes of MOS memory, and a serial line RS-232C interface. Additional capabilities added to the system were a floppy disk system, a nine-track magnetic tape system, an analog-to-digital converter, and a programmable real-time clock. Received signals, E_1 and E_2, were sampled at the point shown in Figure 3 (Section II-C) and input to the ADV11A analog-to-digital converter. Transmitter signals were used for overall timing and sampling intervals. Thus, these techniques are based on the availability of the transmitter signals for use by the receiver, and therefore, are usually limited to monostatic radar configurations.

2. Signal Modeling

A bandpass signal can be written as

$$E(t) = A(t) \cos [\omega_c t - \phi(t)] , \qquad (B\text{-}1)$$

where A(t) is an envelope signal with energy only in a frequency band $f_\omega << f_c$ (Wozencraft and Jacobs, 1965). $\phi(t)$ is the phase function which specifies frequency deviation from the carrier. Assuming the signal does not have significant frequency modulation (i.e., a fixed phase

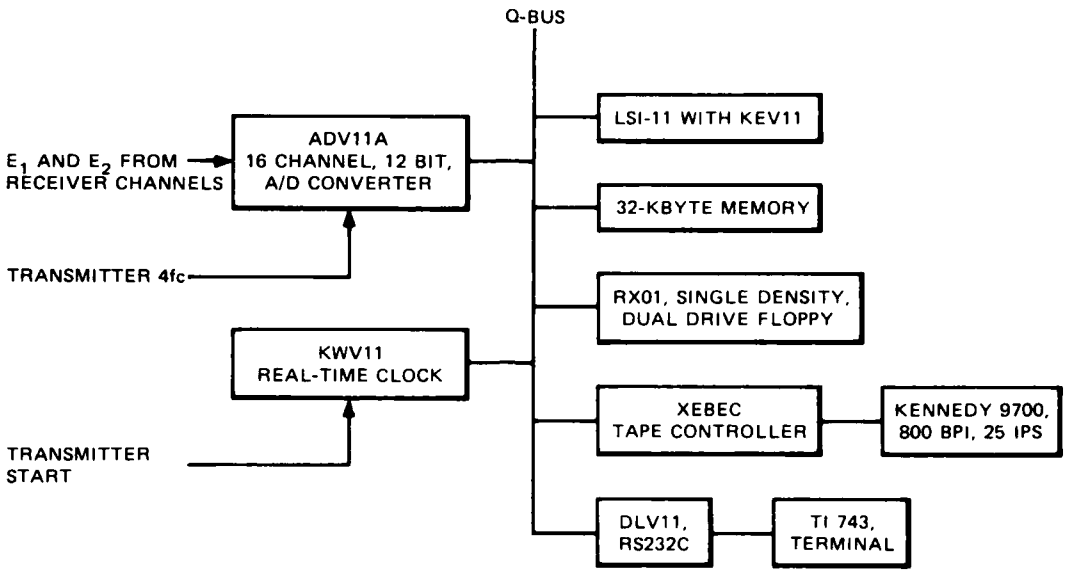

FIGURE B-1 DIGITAL SIGNAL PROCESSING SYSTEM

delay ϕ), trigonometric identities allow E(t) to be decomposed into two terms:

$$E(t) = I(t) \cos(\omega_c t) + Q(t) \sin(\omega_c t) , \qquad (B-2)$$

where

$$I(t) \equiv A(t) \cos \phi , \qquad (B-3)$$

$$Q(t) \equiv A(t) \sin \phi .$$

I(t) is called the in-phase component and Q(t) the quadrature component. I(t) and Q(t) are lowpass signals with bandwidth f_ω. By synchronously sampling E(t), the envelope of the received signal can be analyzed with filters at baseband [using I(t) and Q(t)] instead of filters designed near the carrier frequency (McBride, 1973). This greatly reduces both the storage requirement and computational time needed to implement any digital signal-processing functions. The improvement is approximately

(f_c/f_ω). For the present experiments, $f_c \cong 1600$ Hz and $f_w \cong 100$ Hz. Thus, a reduction of 16 is achieved.

Assume the receiver channel is sampled with a period $T_s = (1/4)T_c$, where $T_c = 1/f_c = 2\pi/\omega_c$. The four samples in time T_c are:

$$E_s(0) = I(0)$$

$$E_s(T_s) = Q(T_s)$$

$$E_s(2T_s) = -I(2T_s)$$

$$E_s(3T_s) = -Q(3T_s) \quad . \tag{B-4}$$

This sampling process can be represented in a phase plane where one revolution of the received signal vector corresponds to T_c; E(t) is sampled four times during T_c. Assuming a phase delay of zero, the four sample points are shown in Figure B-2. A nonzero phase would rotate the four points in the plane.

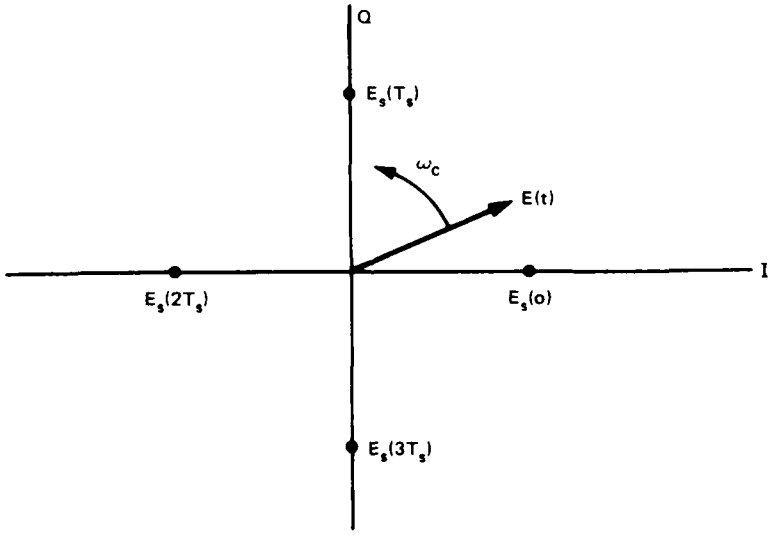

FIGURE B-2 PHASE DIAGRAM FOR SAMPLING OF RECEIVED SIGNAL

Using the series of receiver samples $E_s(i.4T_s)$ and $E\ E_s(i.4T_s + T_s)$ (where $i = 0,1,2,\ldots$ counts the time intervals of length $4T_s = T_c$), the in-phase sequence $I[i]$ is defined as $I(i.4T_s) = I(i.T_c)$, and $Q[i] = Q(i.4T_s + T_s) = Q(i.T_c + T_s)$, the quandrature series. Because $A(t)$ does not appreciably change in T_s, a sampled time series of the envelope can be formed by the in-phase and quandrature series [cf. Eq. (B-3)],

$$A[i] = (I^2[i] + Q^2[i])^{1/2} . \qquad \text{(B-5)}$$

Thus, $I[i]$ and $Q[i]$ contain enough information to specify the sampled envelope of the received signal.

As a test of the ability of synchronous sampling to monitor only signals about the transmitter carrier frequency, a program was written which formed a bandpass filter centered at f_c. The transfer function of this program is shown in Figure B-3. The response was formed by averaging the sampled values from the output of a frequency generator for a 1 s period. The main response is at the transmitter frequency, $f_c = 1550$ Hz. The response at 3100 Hz$(=2f_c)$ results from aliasing. Because the receiver channels include a 16-pole commutating filter, this aliasing response is removed before digital processing during the experiments.

By including the in-phase and quadrature measurements $E(2T_s)$ and $E(3T_s)$, the response at $2f_c$ can be removed digitally and an overall narrower peak at f_c can be achieved. The improved estimates are

$$I[i] = \frac{I(i \cdot 4T_s) - I(i \cdot 4T_s + 2T_s)}{2}$$

$$Q[i] = \frac{Q(i \cdot 4T_s + T_s) - Q(i \cdot 4T_s + 3T_s)}{2} . \qquad \text{(B-6)}$$

However, because these estimates require twice the storage and because the commutating filter minimizes the aliasing effects, they were not used in the digital processing of the receiver channels.

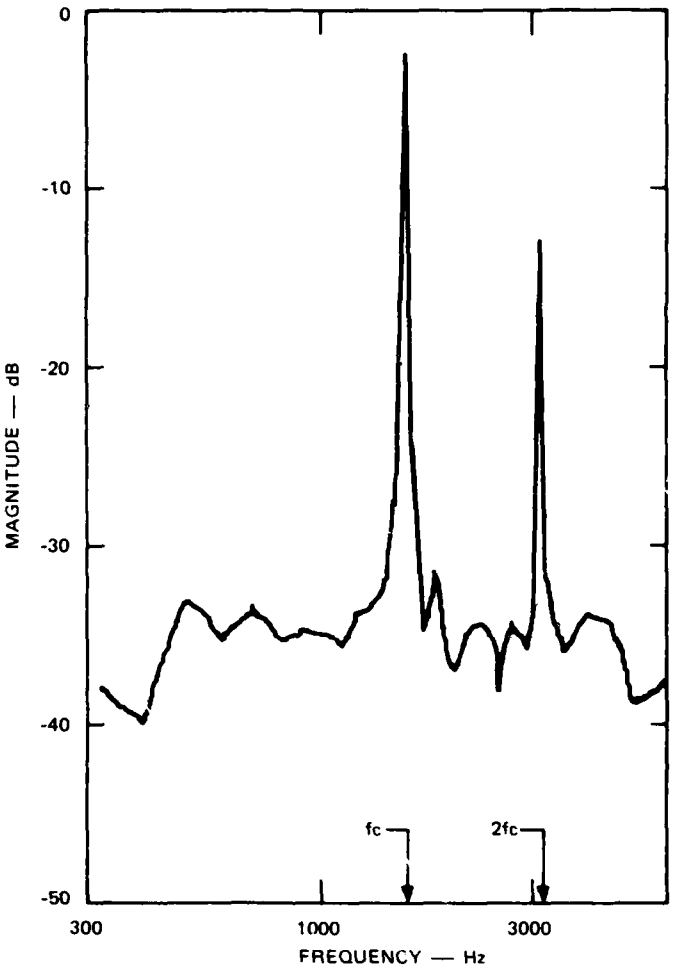

FIGURE B-3 FREQUENCY RESPONSE OF SYNCHRONOUS DEMODULATED FILTER

3. Angle-of-Arrival Estimates

Table B-1 describes the sequential steps of a computer program that calculates wind estimates. An operator inputs the height of the region to be studied along with the width of the transmitter pulse, usually 0.1 s. The computer then waits for a trigger from the transmitter indicating that the pulse has been transmitted. After a time delay equivalent to the propagation time of the pulse from the transmitter to the

Table B-1

A REAL-TIME COMPUTER PROGRAM FOR THE AMPLITUDE TECHNIQUE OF ANGLE-OF-ARRIVAL ESTIMATION

Input height and transmitter pulse duration

Delay (2*height)/velocity after transmitter trigger

Synchronously sample receiver channels for duration of pulse

Average the in-phase and quadrature components of channel 1 and 2,

$$I_1,\ Q_1,\ I_2,\ Q_2$$

Calculate $A_1 = (I_1^2 + Q_1^2)^{1/2}$ and $A_2 = (I_2^2 + Q_2^2)^{1/2}$

Output function $f_1 = \dfrac{A_1 - A_2}{A_1 + A_2}$

"Invert" the function into angle estimate using premeasured f_1 vs θ curve

specified height and back to the receiver, the computer samples the receiver channels for the duration of the pulse width. The program then computes the amplitude angle-of-arrival estimate using the function f_1 of Eq. (9) (Barton, 1970; Carpentier, 1968).

Amplitude monopulse assumes that the two signals being processed from the target are in phase but have different amplitudes. It is an easier design problem to obtain two amplification channels with the same phase delay (especially when using a narrowband filter) than to obtain two channels having the same gain. However, the sequential sampling of the two channels introduces a phase difference resulting from the time delay in the A/D converter (a single sample/hold circuit with an analog multiplexer input), which makes phase measurements difficult.

The time delay contains two parts:

- A fixed delay resulting from the execution of machine instructions and the fixed conversion time of the A/D unit using a successive approximation technique.
- A variable delay resulting from the asynchronous timing between the computer clock and the A/D clock.

The fixed time delay is 54 μs, an equivalent phase delay of 31^{o} at the transmitter frequency. The variable time delay ranges from 0 to 4 μs, a maximum phase delay of 2.3^{o}.

The fixed and variable delay is of little consequence with amplitude measurements, because it is assumed that the amplitude does not change appreciably during this short time. Because part of the delay is fixed, it is possible for a phase measurement program to compensate for this delay. However, with a phase measurement system, the error resulting from the variable phase delay could be significant. Thus, it is important for phase measurement systems to use A/D converters with multichannel sample/hold circuits, which simultaneously make analog measurements and then are sequentially converted into digital values.

During the execution of the amplitude measurement program, an operator had to input the height of the desired region. This was usually the height of an inversion layer which was being displayed by a nearby facsimile recorder using the analog sum of both receiver channel amplitudes. Difficulty in reading the correct height of inversions led to a preface segment in the program which monitored the strengths of echoes for a single transmitter pulse. The height of the region of maximum return was output to the operator and also used as input by the angle-of-arrival program during the next transmitter pulse. Memory limitations allowed only sampling every 50 meters in the vertical, thus it was possible to miss the area of maximum return. This caused a large variation in the angle-of-arrival estimates due to weak signal returns.

Appendix C

LIST OF PARTICIPATING SCIENTIFIC PERSONNEL

Appendix C

LIST OF PARTICIPATING SCIENTIFIC PERSONNEL

Dr. Philip D. Russell, Senior Physicist

Dr. Edward M. Liston, Senior Engineer

Dr. Stephen A. DeLateur, Research Engineer

Dr. Roger S. Vickers, Senior Physicist

Dr. Gerhard Peters (consultant)

Mr. Henry D. Olson, Senior Research Engineer

Dr. Norman J.F. Chang, Senior Research Engineer

Mr. Walter Jimison, Research Engineer

Mr. William Dyer, Engineering Assistant

Mr. William Evans, Staff Scientist

Mr. Ronald Presnell, Senior Research Engineer

Dr. Vicent Salmon, Staff Scientist

No advanced degrees were earned by any personnel while employed on this project.

REFERENCES

Air Weather Service, 1971: "Impact of Low-Level Wind Estimates on the Success of Paradrop Missions," special study, Directorate of Aerospace Services, DCS/Aerospace Sci.; Scott Air Force Base, Illinois, 1971.

Barton, K., ed., 1970: Radars, Volume 1: Monopulse Radar. (Artech House, Dedham, Massachusetts).

Beran, D.W., 1974: "Remote Sensing Wind and Wind Shear System," Report FAA-RD-74-3, Department of Transportation, FAA, Washington, D.C., 20591.

Beran, D.W., B.C. Willmarth, F.C. Carsey, and F.F. Hall, Jr., 1974: "An Acustic-Doppler Wind Measuring System," J. Acoust. Soc. Am., Vol. 55, pp. 334-338.

Carpentier, M.H., 1968: Radars: New Concepts. Ch. 6 (Gordon and Breach, New York).

Cormier, R.V., 1975: "The Horizontal Variability of Vertically Integrated Boundary Layer Winds," J. Geophys. Res., Vol. 80, pp. 3407-3409.

Georges, T.M., and S.F. Clifford, 1972: "Acoustic Sounding in a Refracting Atmosphere," J. Acoust. Soc. Am., Vol. 52, pp. 1397-1405.

Hall, F.F., 1972: "Temperature and Wind Structure Studies by Acoustic Echo Sounding," in Remote Sensing of the Troposphere, V.E. Derr, ed., pp. 18.1-18.26 (U.S. Government Printing Office, Washington, D.C.).

Hall, F.F., J.G. Edinger, and W.D. Neff, 1975: "Convective Plumes in the Planetary Boundary Layer, Investigated with an Acoustic Sounder," J. Appl. Meteor., Vol. 14, pp. 513-523.

Mahoney, A.R., 1974: "Acoustic Angle-of-Arrival Wind Sensing Technique," In Internal Report No. FAA-RD-74-3 (DOT/FAA Systems Res. Dev. Office, Washington, D.C.).

McAllister, L.G., 1971a: "Acoustic Radar Sounding of the Lower Atmosphere," NASATM 4-62, 150, Proceedings Workshop, Ames Research Center, 12-16 July.

McAllister, L.G., 1971b: "Wind Velocity Measurements in the Lower Atmosphere Using Acoustic Sounding Techniques," WRE Technical Note A204 (AP), Department of Supply, Australian Defense Scientific Service, Weapons Research Establishment, Salisbury, South Australia.

McBride, A.L., 1973: "On Optimum Sampled-Data FM Demodulation," IEEE Trans. Comm., Vol. COM-21, pp. 40-50.

Peters, G., C. Wamser, and H. Hinzpeter, 1978: "Acoustic Doppler and Angle of Arrival Wind Detection and Comparisons with Direct Measurements at 300-m Mast," J. Appl. Meteor., Vol. 17, pp. 1171-1178.

Rhodes, D.R., 1959: Introduction to Monopulse, (McGraw-Hill Book Company, New York, New York).

Skolnick, M.I., ed., 1970: Radar Handbook (McGraw-Hill Book Company, New York, New York).

Swingle, D.M.: "The Army's Automatic Meteorological System," Technical Report 217, Proceedings of the 5th AWS Technical Exchange Conf., Air Force Academy, 14-17 July 1969.

Wozencraft, J.M. and I.M. Jacobs, 1965: Principles of Communication Engineering (John Wiley, and Sons, New York, New York).

Wycoff, F.J., D.W. Beran, and F.F. Hall, Jr., 1973: "A Comparison of the Low Level Radiosonde and the Acoustic Echo Sounder for Monitoring Atmospheric Stability," J. Appl. Meteor., Vol. 12, pp. 1192-1204.

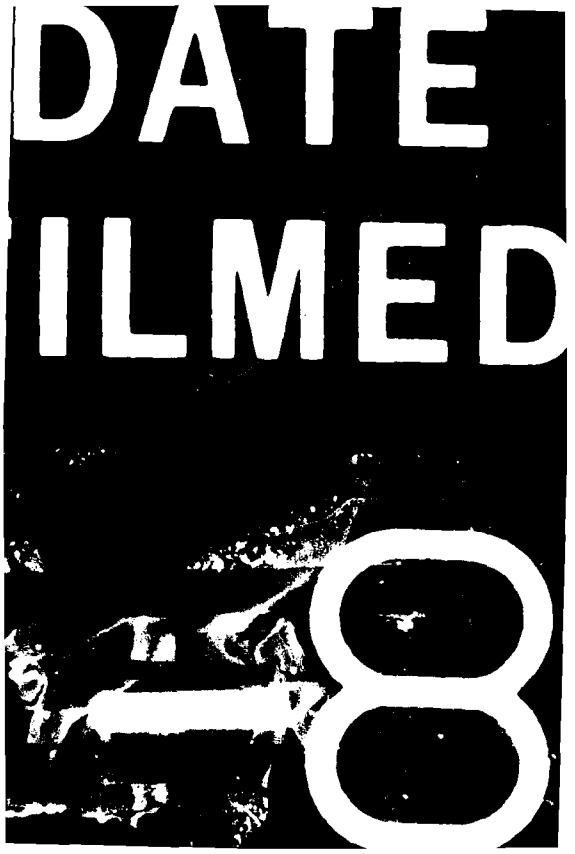
DATE
ILMED
8